

PDF hosted at the Radboud Repository of the Radboud University Nijmegen

The following full text is a publisher's version.

For additional information about this publication click this link.

<http://hdl.handle.net/2066/129145>

Please be advised that this information was generated on 2017-12-05 and may be subject to change.

Determination of α_s for b quarks at the Z^0 resonance

DELPHI Collaboration

P. Abreu^t, W. Adam^g, T. Adye^{ak}, E. Agasi^{ad}, R. Aleksan^{am}, G.D. Alekseevⁿ, A. Algeri^m, P. Allen^{aw}, S. Almedhed^w, S.J. Alvsvaag^d, U. Amaldi^g, A. Andreazza^{aa}, P. Antilogus^x, W.-D. Apel^o, R.J. Apsimon^{ak}, Y. Arnoud^{am}, B. Åsman^{as}, J.-E. Augustin^r, A. Augustinus^{ad}, P. Baillon^g, P. Bambade^r, F. Barao^t, R. Barate^l, G. Barbiellini^{au}, D.Y. Bardinⁿ, G.J. Barker^{ah}, A. Baroncelli^{ao}, O. Barring^g, J.A. Barrio^y, W. Bartl^{ay}, M.J. Bates^{ak}, M. Battaglia^m, M. Baubillier^v, K.-H. Becks^{ba}, C.J. Beeston^{ah}, M. Begalli^{aj}, P. Beilliere^f, Yu. Belokopytov^{aq}, P. Beltran^l, D. Benedic^h, A.C. Benvenuti^e, M. Berggren^r, D. Bertrand^b, F. Bianchi^{at}, M.S. Bilenkyⁿ, P. Billoir^v, J. Bjarne^w, D. Bloch^h, S. Blyth^{ah}, V. Bocci^{al}, P.N. Bogolubovⁿ, T. Bolognese^{am}, M. Bonesini^{aa}, W. Bonivento^{aa}, P.S.L. Booth^u, G. Borisov^{aq}, H. Borner^g, C. Bosio^{ao}, B. Bostjancic^{ar}, S. Bosworth^{ah}, O. Botner^{av}, B. Bouquet^r, C. Bourdarios^r, T.J.V. Bowcock^u, M. Bozzo^k, S. Braibant^b, P. Branchini^{ao}, K.D. Brand^{ai}, R.A. Brenner^g, H. Briand^v, C. Bricman^b, R.C.A. Brown^g, N. Brummer^{ad}, J.-M. Brunet^f, L. Bugge^{af}, T. Buran^{af}, H. Burmeister^g, J.A.M.A. Buytaert^g, M. Caccia^g, M. Calvi^{aa}, A.J. Camacho Rozas^{ap}, R. Campion^u, T. Camporesi^g, V. Canale^{al}, F. Cao^b, F. Carena^g, L. Carroll^u, C. Caso^k, M.V. Castillo Gimenez^{aw}, A. Cattai^g, F.R. Cavallo^e, L. Cerrito^{al}, V. Chabaud^g, A. Chan^a, Ph. Charpentier^g, L. Chaussard^r, J. Chauveau^v, P. Checchia^{at}, G.A. Chelkovⁿ, L. Chevalier^{am}, P. Chliapnikov^{aq}, V. Chorowicz^v, J.T.M. Chrin^{aw}, P. Collins^{ah}, J.L. Contreras^y, R. Contri^k, E. Cortina^{aw}, G. Cosme^r, F. Couchot^r, H.B. Crawley^a, D. Crennell^{ak}, G. Crosetti^k, M. Crozon^f, J. Cuevas Maestro^{ag}, S. Czellar^m, E. Dahl-Jensen^{ab}, B. Dalmagne^r, M. Dam^{af}, G. Damgaard^{ab}, E. Daubie^b, A. Daum^o, P.D. Dauncey^{ah}, M. Davenport^g, P. David^v, J. Davies^u, W. Da Silva^v, C. Defoix^f, P. Delpierre^f, N. Demaria^{at}, A. De Angelis^{au}, H. De Boeck^b, W. De Boer^o, C. De Clercq^b, M.D.M. De Fez Laso^{aw}, N. De Groot^{ad}, C. De La Vaissiere^v, B. De Lotto^{au}, A. De Min^{aa}, H. Dijkstra^g, L. Di Ciaccio^{al}, J. Dolbeau^f, M. Donszelmann^g, K. Doroba^{az}, M. Dracog^g, J. Drees^{ba}, M. Dris^{ae}, Y. Dufour^g, F. Dupont^l, D. Edsall^a, L.-O. Eek^{av}, P.A.-M. Eerola^g, R. Ehret^o, T. Ekelof^{av}, G. Ekspong^{as}, A. Elliot Peisert^{ai}, J.-P. Engel^h, N. Ershaidat^v, D. Fassouliotis^{ae}, M. Feindt^g, M. Fernandez Alonso^{ap}, A. Ferrer^{aw}, T.A. Filippas^{ae}, A. Firestone^a, H. Foeth^g, E. Fokitis^{ae}, F. Fontanelli^k, K.A.J. Forbes^u, J.-L. Fousset^z, S. Francon^x, B. Franek^{ak}, P. Frenkiel^f, D.C. Fries^o, A.G. Frodesen^d, R. Fruhwirth^{ay}, F. Fulda-Quenzer^r, K. Furnival^u, H. Furstenau^o, J. Fuster^g, D. Gamba^{at}, C. Garcia^{aw}, J. Garcia^{ap}, C. Gaspar^g, U. Gasparini^{ai}, Ph. Gavillet^g, E.N. Gazis^{ae}, J.-P. Gerber^h, P. Giacomelli^g, R. Gokieli^{az}, B. Golob^{ar}, V.M. Golovatyukⁿ, J.J. Gomez Y Cadenas^g, G. Gopal^{ak}, M. Gorski^{az}, V. Gracco^k, A. Grant^g, F. Grard^b, E. Graziani^{ao}, G. Grosdidier^r, E. Gross^g, P. Grosse-Wiesmann^g, B. Grossetete^v, S. Gumenyuk^{aq}, J. Guy^{ak}, U. Haedinger^o, F. Hahn^{ba}, M. Hahn^o, S. Haider^{ad}, A. Hakansson^w, A. Hallgren^{av}, K. Hamacher^{ba}, G. Hamel De Monchenault^{am}, W. Hao^{ad}, F.J. Harris^{ah}, V. Hedberg^w, T. Henkes^g, J.J. Hernandez^{aw}, P. Herquet^b, H. Herr^g, T.L. Hessing^u, I. Hietanen^m, C.O. Higgins^u, E. Higon^{aw}, H.J. Hilke^g, S.D. Hodgson^{ah}, T. Hofmohl^{az}, R. Holmes^a, S.-O. Holmgren^{as}, D. Holthuisen^{ad}, P.F. Honore^f, J.E. Hooper^{ab}, M. Houlden^u, J. Hrubec^{av}, K. Huet^b, P.O. Hulth^{as}, K. Hultqvist^{as}, P. Ioannou^c, P.-S. Iversen^d,

J.N. Jackson^u, P. Jalocho^p, G. Jarlskog^w, P. Jarry^{am}, B. Jean-Marie^r, E.K. Johansson^{as}, D. Johnson^u, M. Jonker^g, L. Jonsson^w, P. Juillot^h, G. Kalkanis^c, G. Kalmus^{ak}, F. Kapusta^v, M. Karlsson^g, E. Karvelas^l, S. Katsanevas^c, E.C. Katsoufis^{ae}, R. Keranen^g, J. Kesteman^b, B.A. Khomenkoⁿ, N.N. Khovanskiⁿ, B. King^u, N.J. Kjaer^g, H. Klein^g, A. Klovning^d, P. Kluit^{ad}, A. Koch-Mehrin^{ba}, J.H. Koehne^o, B. Koene^{ad}, P. Kokkinias^l, M. Koratzinos^{af}, A.V. Korytovⁿ, V. Kostioukhine^{aq}, C. Kourkoumelis^c, O. Kouznetsovⁿ, P.H. Kramer^{ba}, J. Krolkowski^{az}, I. Kronkvist^w, U. Kruener-Marquis^{ba}, W. Krupinski^p, K. Kulka^{av}, K. Kurvinen^m, C. Lacasta^{aw}, C. Lambropoulos^l, J.W. Lamsa^a, L. Lanceri^{au}, V. Lapin^{aq}, J.-P. Laugier^{am}, R. Lauhakangas^m, G. Leder^{ay}, F. Ledroit^l, R. Leitner^{ac}, Y. Lemoigne^{am}, J. Lemonne^b, G. Lenzen^{ba}, V. Lepeltier^r, T. Lesiak^p, J.M. Levy^h, E. Lieb^{ba}, D. Liko^{ay}, J. Lindgren^m, R. Lindner^{ba}, A. Lipniacka^{az}, I. Lippi^{ai}, B. Loerstad^w, M. Lokajicek^j, J.G. Loken^{ah}, A. Lopez-Fernandez^g, M.A. Lopez Aguera^{ap}, M. Los^{ad}, D. Loukas^l, J.J. Lozano^{aw}, P. Lutz^f, L. Lyons^{ah}, G. Maehlum^{af}, J. Maillard^f, A. Maio^l, A. Maltezos^l, F. Mandl^{ay}, J. Marco^{ap}, M. Margoni^{ai}, J.-C. Marin^g, A. Markou^l, T. Maron^{ba}, S. Marti^{aw}, L. Mathis^a, F. Matorras^{ap}, C. Matteuzzi^{aa}, G. Matthiae^{af}, M. Mazzucato^{ai}, M. Mc Cubbin^u, R. Mc Kay^a, R. Mc Nulty^u, G. Meola^k, C. Meroni^{aa}, W.T. Meyer^a, M. Michelotto^{ai}, I. Mikulec^{ay}, L. Mirabito^x, W.A. Mitaroff^{ay}, G.V. Mitselmakherⁿ, U. Mjoernmark^w, T. Moa^{as}, R. Moeller^{ab}, K. Moenig^g, M.R. Monge^k, P. Morettini^k, H. Mueller^o, W.J. Murray^{ak}, B. Muryn^p, G. Myatt^{ah}, F.L. Navarria^e, P. Negri^{aa}, R. Nicolaidou^c, B.S. Nielsen^{ab}, B. Nijjhar^u, V. Nikolaenko^{aq}, P.E.S. Nilsen^d, P. Niss^{as}, A. Nomerotski^{ai}, V. Obraztsov^{aq}, A.G. Olshevskiⁿ, R. Orava^m, A. Ostankov^{aq}, K. Osterberg^m, A. Ouraou^{am}, M. Paganoni^{aa}, R. Pain^v, H. Palka^p, Th.D. Papadopoulou^{ae}, L. Pape^g, F. Parodi^k, A. Passeri^{ao}, M. Pegoraro^{ai}, J. Pennanen^m, L. Peralta^l, H. Pernegger^{ay}, M. Pernicka^{ay}, A. Perrotta^e, C. Petridou^{au}, A. Petrolini^k, O. Petrovykh^{aq}, F. Pierre^{am}, M. Pimenta^l, O. Pingot^b, S. Plaszczynski^r, O. Podobrin^o, M.E. Pol^q, G. Polok^p, P. Poropat^{au}, V. Pozdniakovⁿ, P. Privitera^o, A. Pullia^{aa}, D. Radojicic^{ah}, S. Ragazzi^{aa}, H. Rahmani^{ae}, P.N. Ratoff^s, A.L. Read^{af}, P. Rebecchi^g, N.G. Redaelli^{aa}, M. Regler^{ay}, D. Reid^g, P.B. Renton^{ah}, L.K. Resvanis^c, F. Richard^r, M. Richardson^u, J. Ridky^j, G. Rinaudo^{at}, I. Roditi^q, A. Romero^{at}, I. Roncagliolo^k, P. Ronchese^{ai}, C. Ronnqvist^m, E.I. Rosenberg^a, S. Rossi^g, E. Rosso^g, P. Roudeau^r, T. Rovelli^c, W. Ruckstuhl^{ad}, V. Ruhlmann-Kleider^{am}, A. Ruiz^{ap}, K. Rybicki^p, H. Saarikko^m, Y. Sacquin^{am}, G. Sajot^l, J. Salt^{aw}, J. Sanchez^y, M. Sannino^{k,an}, S. Schael^g, H. Schneider^o, M.A.E. Schyns^{ba}, G. Sciolla^{at}, F. Scuri^{au}, A.M. Segar^{ah}, A. Seitz^o, R. Sekulin^{ak}, M. Sessa^{au}, G. Sette^k, R. Seufert^o, R.C. Shellard^{aj}, I. Siccama^{ad}, P. Siegrist^{am}, S. Simonetti^k, F. Simonetto^{ai}, A.N. Sisakianⁿ, G. Skjevling^{af}, G. Smadja^{am,x}, N. Smirnov^{aq}, O. Smirnovaⁿ, G.R. Smith^{ak}, R. Sosnowski^{az}, D. Souza-Santos^{aj}, T.S. Spasoff^l, E. Spiriti^{ao}, S. Squarcia^k, H. Staeck^{ba}, C. Stanescu^{ao}, S. Stapnes^{af}, G. Stavropoulos^l, F. Stichelbaut^b, A. Stocchi^r, J. Strauss^{ay}, J. Straver^g, R. Strub^h, B. Stugu^d, M. Szczekowski^g, M. Szeptycka^{az}, P. Szymanski^{az}, T. Tabarelli^{aa}, O. Tchikilev^{aq}, G.E. Theodosiou^l, A. Tilquin^z, J. Timmermans^{ad}, V.G. Timofeevⁿ, L.G. Tkatchevⁿ, T. Todorov^h, D.Z. Toet^{ad}, O. Toker^m, B. Tome^l, E. Torassa^{at}, L. Tortora^{ao}, D. Treille^g, U. Trevisan^k, W. Trischuk^g, G. Tristram^f, C. Troncon^{aa}, A. Tsiros^g, E.N. Tsyganovⁿ, M. Turala^p, M.-L. Turluer^{am}, T. Tuuva^m, I.A. Tyapkin^v, M. Tyndel^{ak}, S. Tzamarias^u, S. Ueberschaer^{ba}, O. Ullaland^g, V. Uvarov^{aq}, G. Valenti^e, E. Vallazza^{at}, J.A. Valls Ferrer^{aw}, C. Vander Velde^b, G.W. Van Apeldoorn^{ad}, P. Van Dam^{ad}, M. Van Der Heijden^{ad}, W.K. Van Doninck^b, P. Vaz^g, G. Vegni^{aa}, L. Ventura^{ai}, W. Venus^{ak}, F. Verbeure^b, M. Verlato^{ai}, L.S. Vertogradovⁿ, D. Vilanova^{am}, P. Vincent^x, L. Vitale^m, E. Vlasov^{aq}, A.S. Vodopyanovⁿ, M. Vollmer^{ba}, M. Voutilainen^m, V. Vrba^{ao}, H. Wahlen^{ba}, C. Walck^{as}, F. Waldner^{au}, M. Wayne^a, A. Wehr^{ba}, M. Weierstall^{ba}, P. Weilhammer^g, J. Werner^{ba},

A.M. Wetherell^g, J.H. Wickens^b, G.R. Wilkinson^{ah}, W.S.C. Williams^{ah}, M. Winter^h,
 M. Witek^p, G. Wormser^r, K. Woschnagg^{av}, N. Yamdagni^{as}, P. Yepes^g, A. Zaitsev^{aq},
 A. Zalewska^p, P. Zalewski^r, D. Zavrtnik^{ar}, E. Zevgolatakos^l, G. Zhang^{ba}, N.I. Ziminⁿ,
 M. Zito^{am}, R. Zuberi^{ah}, R. Zukanovich Funchal^f, G. Zumerle^{ai} and J. Zuniga^{aw}

^a Ames Laboratory and Department of Physics, Iowa State University, Ames, IA 50011, USA

^b Physics Department, Univ. Instelling Antwerpen, Universiteitsplein 1, B-2610 Wilrijk, Belgium
 and IIHE, ULB-VUB, Pleinlaan 2, B-1050 Brussels, Belgium

and Faculté des Sciences, Univ. de l'Etat Mons, Av. Maistriau 19, B-7000 Mons, Belgium

^c Physics Laboratory, University of Athens, Solonos Str 104, GR-10680 Athens, Greece

^d Department of Physics, University of Bergen, Allégaten 55, N-5007 Bergen, Norway

^e Dipartimento di Fisica, Università di Bologna and INFN, Via Irnerio 46, I-40126 Bologna, Italy

^f Collège de France, Lab de Physique Corpusculaire, IN2P3-CNRS, F-75231 Paris Cedex 05, France

^g CERN, CH-1211 Geneva 23, Switzerland

^h Centre de Recherche Nucléaire, IN2P3 - CNRS/ULP, BP20, F-67037 Strasbourg Cedex, France

ⁱ Institute of Nuclear Physics, N.C.S.R. Demokritos, P.O. Box 60228, GR-15310 Athens, Greece

^j FZU, Inst of Physics of the C.A.S. High Energy Physics Division, Na Slovance 2, CS-180 40, Praha 8, Czech Republic

^k Dipartimento di Fisica, Università di Genova and INFN, Via Dodecaneso 33, I-16146 Genova, Italy

^l Institut des Sciences Nucléaires, IN2P3-CNRS, Université de Grenoble 1, F-38026 Grenoble, France

^m Research Institute for High Energy Physics, SEFT, Siltavuorenpenger 20 C, SF-00170 Helsinki, Finland

ⁿ Joint Institute for Nuclear Research, Dubna, Head Post Office, P.O. Box 79, 101 000 Moscow, Russian Federation

^o Institut für Experimentelle Kernphysik, Universität Karlsruhe, Postfach 6980, W-7500 Karlsruhe 1, Germany

^p High Energy Physics Laboratory, Institute of Nuclear Physics, Ul. Kawory 26 a, PL-30055 Krakow 30, Poland

^q Centro Brasileiro de Pesquisas Físicas, rua Xavier Sigaud 150, RJ-22290 Rio de Janeiro, Brazil

^r Université de Paris-Sud, Lab de l'Accélérateur Linéaire, IN2P3-CNRS, Bat 200, F-91405 Orsay, France

^s School of Physics and Materials, University of Lancaster, Lancaster LA1 4YB, UK

^t LIP, IST, FCUL - Av. Elias Garcia, 14 - 1º, P-1000 Lisboa Codex, Portugal

^u Department of Physics, University of Liverpool, P.O. Box 147, Liverpool L69 3BX, UK

^v LPNHE, IN2P3-CNRS, Universités Paris VI et VII, Tour 33 (RdC), 4 place Jussieu, F-75252 Paris Cedex 05, France

^w Department of Physics, University of Lund, Sölvegatan 14, S-22363 Lund, Sweden

^x Université Claude Bernard de Lyon, IPNL, IN2P3-CNRS, F-69622 Villeurbanne Cedex, France

^y Universidad Complutense, Avda Complutense s/n, E-28040 Madrid, Spain

^z Univ d'Aix - Marseille II - CPP, IN2P3-CNRS, F-13288 Marseille Cedex 09, France

^{aa} Dipartimento di Fisica, Università di Milano and INFN, Via Celoria 16, I-20133 Milan, Italy

^{ab} Niels Bohr Institute, Blegdamsvej 17, DK-2100 Copenhagen Ø, Denmark

^{ac} NC, Nuclear Centre of MFF, Charles University, Areal MFF, V Holesovickach 2, CS-180 00, Praha 8, Czech Republic

^{ad} NIKHEF-H, Postbus 41882, NL-1009 DB Amsterdam, The Netherlands

^{ae} National Technical University, Physics Department, Zografou Campus, GR-15773 Athens, Greece

^{af} Physics Department, University of Oslo, Blindern, N-1000 Oslo 3, Norway

^{ag} Dpto. Fisica, Univ. Oviedo, C/P Jimenez Casas, S/N-33006 Oviedo, Spain

^{ah} Department of Physics, University of Oxford, Keble Road, Oxford OX1 3RH, UK

^{ai} Dipartimento di Fisica, Università di Padova and INFN, Via Marzolo 8, I-35131 Padua, Italy

^{aj} Depto. de Fisica, Pontificia Univ Católica, C.P. 38071 RJ-22453 Rio de Janeiro, Brazil

^{ak} Rutherford Appleton Laboratory, Chilton, Didcot OX11 0QX, UK

^{al} Dipartimento di Fisica, Università di Roma II and INFN, Tor Vergata, I-00173 Rome, Italy

^{am} Centre d'Etude de Saclay, DSM/DAPNIA, F-91191 Gif-sur-Yvette Cedex, France

^{an} Dipartimento di Fisica, Università di Salerno, I-84100 Salerno, Italy

^{ao} Istituto Superiore di Sanità, Ist Naz di Fisica Nucl (INFN), Viale Regina Elena 299, I-00161 Rome, Italy

^{ap} C.E.A.F.M., C.S.I.C., Univ Cantabria, Avda. los Castros, S/N-39006 Santander, Spain

^{aq} Inst. for High Energy Physics, Serpukov P O Box 35, Protvino (Moscow Region), Russian Federation

^{ar} J. Stefan Institute and Department of Physics, University of Ljubljana, Jamova 39, SI-61000 Ljubljana, Slovenia

^{as} Institute of Physics, University of Stockholm, Vanadisvägen 9, S-113 46 Stockholm, Sweden

^{at} Dipartimento di Fisica Sperimentale, Università di Torino and INFN, Via P. Giuria 1, I-10125 Turin, Italy

^{au} Dipartimento di Fisica, Università di Trieste and INFN, Via A. Valerio 2, I-34127 Trieste, Italy

and Istituto di Fisica, Università di Udine, I-33100 Udine, Italy

^{av} Department of Radiation Sciences, University of Uppsala, P.O. Box 535, S-751 21 Uppsala, Sweden

^{aw} IFIC, Valencia-CSIC, and D.F.A.M.N., U. de Valencia, Avda. Dr. Moliner 50, E-46100 Burjassot (Valencia), Spain

^{ay} Institut für Hochenergiephysik, Österr. Akad. d. Wissensch., Nikolsdorfergasse 18, A-1050 Vienna, Austria

^{az} Inst. Nuclear Studies and University of Warsaw, Ul. Hoza 69, PL-00681 Warsaw, Poland

^{ba} Fachbereich Physik, University of Wuppertal, Postfach 100 127, W-5600 Wuppertal 1, Germany

Received 19 April 1993

Editor: L. Montanet

The strong coupling constant for b quarks has been determined, and its flavour independence, as predicted by QCD, investigated. The analysis involved events with lepton candidates selected from approximately 356 000 hadronic decays of the Z^0 , collected by the DELPHI detector at LEP in 1990 and 1991. A method based on a direct comparison of the three-jet fraction in a b enriched sample, selected by requiring leptons with large momenta and transverse momenta, to that of the entire hadronic sample, illustrated the significant effect of the b quark mass on the multi-jet cross section, and verified the flavour independence of the strong coupling constant to an accuracy of $\pm 6\%$. A second procedure based on a fit to the momentum and transverse momentum spectra of the lepton candidates in both two-jet and three (or more)-jet event samples simultaneously determined the b content in each, and, using second order QCD calculations, gave an absolute measurement of α_s for b quarks of 0.118 ± 0.004 (stat.) ± 0.003 (syst.) ± 0.008 (scale). A comparison with α_s for all quark flavours, as measured from the three-jet fraction in all hadronic events, further allowed the coupling strength for b quarks to be expressed in terms relative to that for uds quarks, thereby cancelling certain common systematic uncertainties, and yielded $\alpha_s^b/\alpha_s^{uds} = 1.00 \pm 0.04$ (stat.) ± 0.03 (syst.).

1. Introduction

The strong coupling constant, $\alpha_s(Q^2)$, is, apart from the quark masses, the fundamental parameter of the theory of Quantum Chromodynamics, QCD. Its determination is therefore an important experimental goal with many different methods of analysis being employed [1,2]. Presently the error on α_s , as determined from a study of topological variables [3,4], is 5%, and is dominated by theoretical uncertainties, in particular that due to the renormalization scale.

For the most part, previous analyses have concentrated on a determination of α_s without distinguishing between quark flavours. A further important test of the validity of QCD is to determine the coupling constant for the individual quark flavours as these are predicted by the theory not to differ. The first experiments to address the question of the relative strength of the strong coupling constant of heavy quarks, at centre-of-mass energies between 28 and 46 GeV [5], suffered largely from a lack of statistics and were thus unable to derive any precise conclusions. Better statistical precision was obtained from comparisons of α_s measurements in decay processes of $c\bar{c}$ and $b\bar{b}$ quarkonium states with those in the lower energy continuum, where only the light uds quarks are produced [6]. The energy scales involved, however, are very different to those applicable here. A further indirect method is to

compare the three-jet rate, which is a measure of α_s , at the Z^0 resonance with that at lower centre-of-mass energies where the flavour component of hadrons is very different. Extrapolating the results from lower energies to the Z^0 resonance and then separating the contribution from quarks with different charges, one concludes that the strong coupling constants for u -type and d -type quarks agree to within 10% [7]. More recently, the L3 Collaboration [8] has studied the large yield of b events at the Z^0 resonance, using the semi-leptonic decay of the b as a tag; selecting events containing leptons with large momentum and transverse momentum relative to the nearest jet direction, and comparing the number of three-jet events in this b enriched sample to that of the entire hadronic sample, the error for the relative strong coupling constant for b quarks was reduced to 8%.

In this article, a description is presented of a measurement of the relative strength of the coupling constant for b quarks following a procedure similar to that in ref. [8]. Another approach presented here is to fit the momentum and transverse momentum spectra of the various processes yielding leptons to the corresponding distribution in the two- and three-jet data samples simultaneously. The b component in the two- and three-jet samples can thus be extracted and a measurement for α_s^b obtained. Results adopting this procedure are also presented. The data correspond to

approximately 356 000 selected hadronic Z^0 decays collected during the 1990 and 1991 LEP data taking periods at centre-of-mass energies on or around the Z^0 peak. For the 1991 data, both muon and electron candidates within the hadronic final state have been analysed, while for the 1990 data, only muon candidates have been investigated.

2. The DELPHI detector

The DELPHI detector at the Large Electron Positron collider at CERN has been used to collect a sample of events containing a hadronic final state produced by the decay of the Z^0 into a $q\bar{q}$ pair. A detailed description of the detector, the trigger conditions and the readout system can be found in ref. [9]. Here, only the main components of DELPHI relevant to this analysis are briefly described.

The detector is centred on the interaction point and, in the barrel region, consists of a system of central tracking chambers and an electromagnetic calorimeter, positioned inside a superconducting solenoidal coil which provides a uniform magnetic field of 1.23 T. The central tracking detectors, which include the vertex detector, the inner detector, the time projection chamber (TPC) and the outer detector, measure charged particles with an average momentum resolution of $\sigma(p)/p = 0.001p$ in the polar angle region between 30° and 150° . The tracking of charged tracks in the forward region is supplemented by two systems of drift chambers on either side of the detector. The main tracking element is the TPC, whose 192 sense wires provide a measurement of the energy loss, dE/dx , for charged particles, with a resolution of $\pm 5.5\%$ in dimuon events. The High Density Projection Chamber (HPC) is the barrel electromagnetic calorimeter. The HPC is a gas sampling calorimeter which measures with high granularity the three-dimensional charge distribution induced by electromagnetic showers, enabling the identification of electrons in a hadronic environment. Surrounding the solenoid is the return yoke of the magnet, instrumented with limited streamer chambers to serve as a hadron calorimeter.

The muon detection system is contained within the outer layers of the yoke and beyond. The barrel muon detector consists of three modules of drift

chambers, with each module comprising two active layers, enabling the r, ϕ and z coordinates of penetrating charged particles to be recorded. The muon detection system in both forward regions consists of two modules of drift chambers arranged in quadrants. A module consists of two orthogonal planes of drift chambers with delay line readout, each providing xyz measurements of the penetrating tracks.

3. Selection of hadronic events containing a lepton

The selection of hadronic Z^0 decays was accomplished essentially with charged particles [10], which were retained only if they satisfied the following criteria:

- (a) a distance of closest approach to the event vertex of less than 5 cm in r and 10 cm in z ,
- (b) a measured track length of at least 50 cm,
- (c) a momentum greater than 0.1 GeV/ c ,
- (d) a polar angle in the region between 25° and 155° .

A sample of hadronic decays of Z^0 was then obtained by requiring that:

- (a) the total energy of charged particles in each of the two hemispheres defined with respect to the beam axis was greater than 3 GeV (in calculating the energy, a pion mass was assumed),
- (b) the sum of energies in the two hemispheres exceeded 15 GeV,
- (c) the total number of charged particles with momentum above 0.2 GeV/ c was greater than six,
- (d) the polar angle of the thrust axis was within the region between 40° and 140° .

In addition, events containing charged particles with reconstructed momenta greater than 50 GeV/ c were rejected. The cut on the charged multiplicity of the event reduced the contamination from $\tau^+\tau^-$ events to less than 0.1%. The cut on the polar angle of the thrust axis ensured that events were well contained within the active volume of the detector. The total number of hadronic Z^0 events passing the selection criteria was found to be 84 100 and 181 100 for the 1990 and 1991 data taking periods respectively. Those events in which the muon detection system (or the HPC) was operational were further subjected to the muon (electron) identification procedure.

Muon candidates were selected by requiring that particles detected in the tracking chambers penetrate the hadron calorimeter into the muon detection system. A complete description of the muon detection system and the procedure used in selecting muon candidates appears in refs. [11,12]. The salient features are repeated here for convenience. Charged particle tracks were extrapolated from the outer edge of the tracking chambers to the muon detector, taking into account the energy loss of the particle in the calorimeter and allowing for multiple scattering. All charged particles whose extrapolated tracks were associated with a series of hits in the muon chambers were treated as muon candidates. The analysis was restricted to muon candidates with polar angles in the regions between 25° – 45° , 53° – 88° , 92° – 127° and 135° – 155° , thereby excluding regions with poor geometrical acceptance. After applying these criteria, totals of 4610 and 10 110 events containing muon candidates in the momentum range 4 to 35 GeV/ c were selected in the 1990 and 1991 data samples respectively.

The identification of electrons was achieved by examining the response of the HPC to charged particles, and by the energy loss, dE/dx , measured in the TPC. As the analysis was restricted to the barrel region, only particles with polar angles between 45° and 135° were considered. In a first step the energy of the shower was measured from the total charge deposited in the HPC. The initial electron selection then involved the use of a discriminant analysis in which several variables, V_i , describing the longitudinal and transverse shower profiles in separate samples of electromagnetic and hadronic showers of a given energy, were assigned, by means of Monte Carlo simulation, energy dependent coefficients (or weights), $n_i(E)$, that maximized the separation between the electron signal and hadron background. The set of coefficients which corresponded to the energy that best matched that of the shower, was then applied to the variables obtained from the experimental data, and the products $n_i V_i$ were summed to produce a single canonical variable. Electron candidates were then selected by applying a loose cut on the canonical variable, such that a high efficiency (at the expense of a large background) was maintained, and by requiring a dE/dx greater than 1.3 times that for a minimum ionizing particle. A full description of the electron identification procedure is given in ref. [13]. Finally, to reduce further

the contribution from photon conversions and Dalitz pairs, electron candidates which could be combined with any oppositely charged particle arising from the same secondary vertex to form an invariant mass not exceeding $0.02 \text{ GeV}/c^2$, were removed. After applying these criteria, 7900 events containing electron candidates in the momentum range 3 to 30 GeV/ c were selected in the 1991 data sample.

4. Data analysis

For the purpose of this analysis, the data were categorized into three event samples containing:

- (a) inclusive muon hadronic events,
- (b) inclusive electron hadronic events,
- (c) all hadronic events.

For each event in each of the three samples, charged particles were grouped into jets, using a particular jet finding algorithm, following the general procedure briefly outlined. For each pair (i, j) of particles a scaled mass was calculated from the corresponding four-momentum vectors according to a given definition of the jet resolution variable, y_{ij} , the value of which was required to exceed a certain threshold, y_{cut} , for particles to be resolved into different jets. The pair with smallest y_{ij} which satisfied the condition $y_{ij} < y_{\text{cut}}$ was combined to form one pseudo-particle whose four-momentum was determined using a given recombination scheme. The procedure was repeated until all pairs of particles or pseudo-particles no longer fulfilled the requirement $y_{ij} < y_{\text{cut}}$. The remaining particles or pseudo-particles are referred to as jets. A description of the available jet-finding algorithms, with their corresponding recombination schemes and jet resolution variables, y_{ij} , together with a discussion on their relative merits, appears in ref. [14]. The different possibilities investigated in the course of this analysis are listed in table 1.

The processes yielding lepton candidates in hadronic decays of the Z^0 can be classified into the following categories, i :

- (1) $b \rightarrow \mu, e$,
- (2) $b \rightarrow c \rightarrow \mu, e$,
- (3) $b \rightarrow \tau \rightarrow \mu, e$,
- (4) $c \rightarrow \mu, e$,
- (5) $\pi, K \rightarrow \mu; \pi, \gamma \rightarrow e$,
- (6) hadrons misidentified as leptons.

Table 1

Definition of the jet resolution variable, y_{ij} , and of the recombination schemes for various jet finding algorithms, E_{vis} is the total visible energy of the event, and $p_i \equiv (E_i, \vec{p}_i)$ denotes a 4-vector.

Algorithm	Reference	Resolution, y_{ij}	Recombination
E^0	[15]	$(p_i + p_j)^2 / E_{\text{vis}}^2$	$\vec{p}_k = (E_k / \vec{p}_i + \vec{p}_j) (\vec{p}_i + \vec{p}_j)$ $E_k = E_i + E_j$
P	[16]	$(p_i + p_j)^2 / E_{\text{vis}}^2$	$\vec{p}_k = \vec{p}_i + \vec{p}_j$ $E_k = \vec{p}_k $
Durham (D)	[17]	$2 \min(E_i^2, E_j^2) (1 - \cos \theta_{ij}) / E_{\text{vis}}^2$	$p_k = p_i + p_j$
Geneva (G)	[14]	$8 E_i E_j (1 - \cos \theta_{ij}) / 9 (E_i + E_j)^2$	$p_k = p_i + p_j$

Categories $i = 1$ to 4 are processes yielding 'prompt' leptons, while $i = 5, 6$ are regarded as 'background'.

Owing to the hard fragmentation of the b quark and its large mass, leptons arising from the decay of b -flavoured hadrons are characterized by their large momentum, p , and transverse momentum, p_T , relative to the direction of the parent hadron. Their contribution to the lepton yield can therefore be separated on a statistical basis either by applying kinematic cuts, or by using fitting techniques. In this analysis, both procedures were investigated as they are subject to different systematic uncertainties and are thus able to provide an important cross check of the final result.

In method 1, as in ref. [8], a sample of events enriched in b content was obtained by selecting events with leptons of large p and p_T . The parent hadron direction was estimated by the direction of the axis of the jet to which the lepton is associated; this was determined using the Lund cluster algorithm, LUCCLUS [18], with the parameter, d_{join} , for the cluster distance scale set to $2.5 \text{ GeV}/c$. For the computation of the lepton transverse momentum, the momentum of the jet containing the lepton was re-calculated with the contribution from the lepton itself removed. The transverse momentum of the lepton was then measured with respect to this new jet axis and is represented by the symbol p_T^{exc} . Monte Carlo simulation studies show that the use of p_T^{exc} results in a purer sample of b events when kinematical cuts in the transverse momentum are applied. Having imposed large p and p_T^{exc} cuts, the b purity of this sample was estimated from the Monte Carlo simulation which incorporates parameters obtained from fits to the inclusive lepton data [11]. The corrected fraction of three-jet events in

the inclusive lepton sample was then compared with that of the entire hadronic event sample, in which the fraction of b events has been verified to agree with the Standard Model prediction [11,19–21]. Since the b content in the two samples is known, then the relative coupling strengths can easily be computed.

Method 2 uses a more sophisticated approach. The inclusive lepton data were divided into two-jet and three (or more)-jet event samples, and the predicted spectra of the different processes yielding leptons were fitted to the observed distributions in p and p_T in both samples. In this way the b fraction in each of the two- and three (or more)-jet samples was determined and an absolute measurement for α_s^b obtained by comparing the corrected experimental value to the prediction of the full second order QCD analytical expression, the coefficients for which have been calculated in ref. [16]. Here, in contrast to method 1, the transverse momentum was computed with the lepton included in the jet direction, and is represented by the symbol p_T^{inc} . This definition is preferred in a fitting procedure as it has been shown to reflect better the dynamics of the mass of the heavy quark and to be less correlated with the lepton momentum [22]; these features lead to a more accurate measure of the true p_T with respect to the parent hadron direction and enable the b content to be determined with minimal model dependence.

4.1. Method 1: a comparison of the three-jet fractions in different event samples

By imposing p and p_T^{exc} cuts of $4 \text{ GeV}/c$ and $1.5 \text{ GeV}/c$ respectively for muons, and $3 \text{ GeV}/c$ and $1.5 \text{ GeV}/c$ for electrons, the fractions of b events in the two samples is greatly enhanced. The number of lep-

tons remaining after these cuts is 3480 (1590) in the 1991 (1990) inclusive muon sample and 2190 in the 1991 inclusive electron data. It is estimated from the Monte Carlo simulation program and from fits to the inclusive lepton data [11] that the b contents are $(76 \pm 4)\%$ and $(68 \pm 6)\%$ in the muon and electron samples respectively.

The computed fractions of three-jet events (within a given recombination scheme with a given value for the minimum jet resolution cut-off, y_{cut}) in the two samples were compared with the fraction found in the entire hadronic sample, and the following ratios formed:

$$\frac{R_3(l)}{R_3(\text{had})} = \frac{N_3(l)}{N_{\text{tot}}(l)} \frac{N_{\text{tot}}(\text{had})}{N_3(\text{had})}, \quad l = e \text{ or } \mu,$$

where N_3 refers to the number of three-jet events in a given event sample, and N_{tot} is the total number in that sample.

These ratios were corrected for detector and hadronization effects, for each recombination scheme and for each value of y_{cut} using the Monte Carlo JETSET 7.2 Parton Shower model [18] – (the jet multiplicity at parton level was calculated from the final state partons at the end of the QCD shower).

They can easily be expressed in terms of the contribution from light quarks, R_3^{udsc} , and b quarks, R_3^b , assuming that the strong coupling constant is independent of the flavour of the light quark:

$$\frac{R_3(l)}{R_3(\text{had})} = \frac{R_3^b \beta + R_3^{udsc} \gamma}{R_3^b P_{\text{had}}^b + R_3^{udsc} (1 - P_{\text{had}}^b)},$$

where P_{had}^b is the b content in the hadronic event sample, $(22.0 \pm 0.5)\%$. The β and γ terms are

$$\beta = P_1^b C_1 + P_2^b C_2 + P_3^b C_3 + P_5^b C_5 + P_6^b C_6,$$

$$\gamma = P_4^c C_4 + P_5^{udsc} C_5 + P_6^{udsc} C_6,$$

where P_i^q denotes the contribution of process, i , due to quark flavour, q , to the inclusive lepton sample, as estimated from the Monte Carlo simulation model, such that

$$\sum_{i=1,6} P_i^q = 1.$$

The coefficients, C_i , were required in order to account for the bias introduced by the imposition of the p and

p_T^{exc} cuts of the leptons. Such cuts at detector level were found to inadvertently bias the event sample at the parton shower level, with the p (p_T^{exc}) cut tending to reduce (increase) the corrected three-jet fraction of the inclusive lepton sample. The net correction factors, $C_i = R_3^q(l)/R_3^q$, were determined from Monte Carlo simulation studies as a function of y_{cut} for each of the processes, i , yielding leptons. While they were small for leptons from b decay ($C_1 \approx 0.94$ to 1.0 depending on y_{cut}), they were found to be particularly sensitive to the modelling of background processes in the Monte Carlo simulation model. In view of the apparent sensitivity, a large range of values was assigned to C_5 and C_6 for each y_{cut} . For the 1991 muon sample, typical values were $C_5 \approx 1.5$ to 1.9 and $C_6 \approx 1.1$ to 1.3; the effect of their variation was incorporated into the systematic uncertainty.

The above expression was then solved for the ratio R_3^b/R_3^{udsc} . Fig. 1 displays this ratio, as determined from the combined lepton data, for different recombination schemes and y_{cut} values. It is seen that all four recombination schemes give results that are consistent with one another. The data points, however, have not been corrected for the effect of massive quarks which tends to reduce the three-jet cross section. Recent calculations [23] (which specifically include the Z^0 propagator) based on ‘massive’ matrix elements giving the three and four parton cross section at $O(\alpha_s)$ and $O(\alpha_s^2)$ respectively, predict that for b quarks, the depletion of the three-jet rate is significant. Within the E^0 scheme, for instance, the ratio of the three-jet cross section for b quarks to that for d quarks varies from 0.90 to 0.96 as y_{cut} goes from 0.01 to 0.20. The deviation from unity is somewhat greater than that predicted by the JETSET generator [18] when including the earlier calculations of ref. [24] in which only the photon propagator, in $O(\alpha_s)$, had been considered. The new approach considers the different mass coefficients entering the vector and axial terms of the three-jet production cross section and includes a more complete treatment of the available phase space [25]. The combined effect is a further reduction in the three-jet cross section for b quarks, of approximately 2% on average, with respect to that obtained from JETSET.

In order to extract a measurement of the relative strength of the coupling constants, the predicted ratios R_3^b/R_3^{udsc} were therefore corrected for mass effects. These were incorporated using the $O(\alpha_s)$ and $O(\alpha_s^2)$

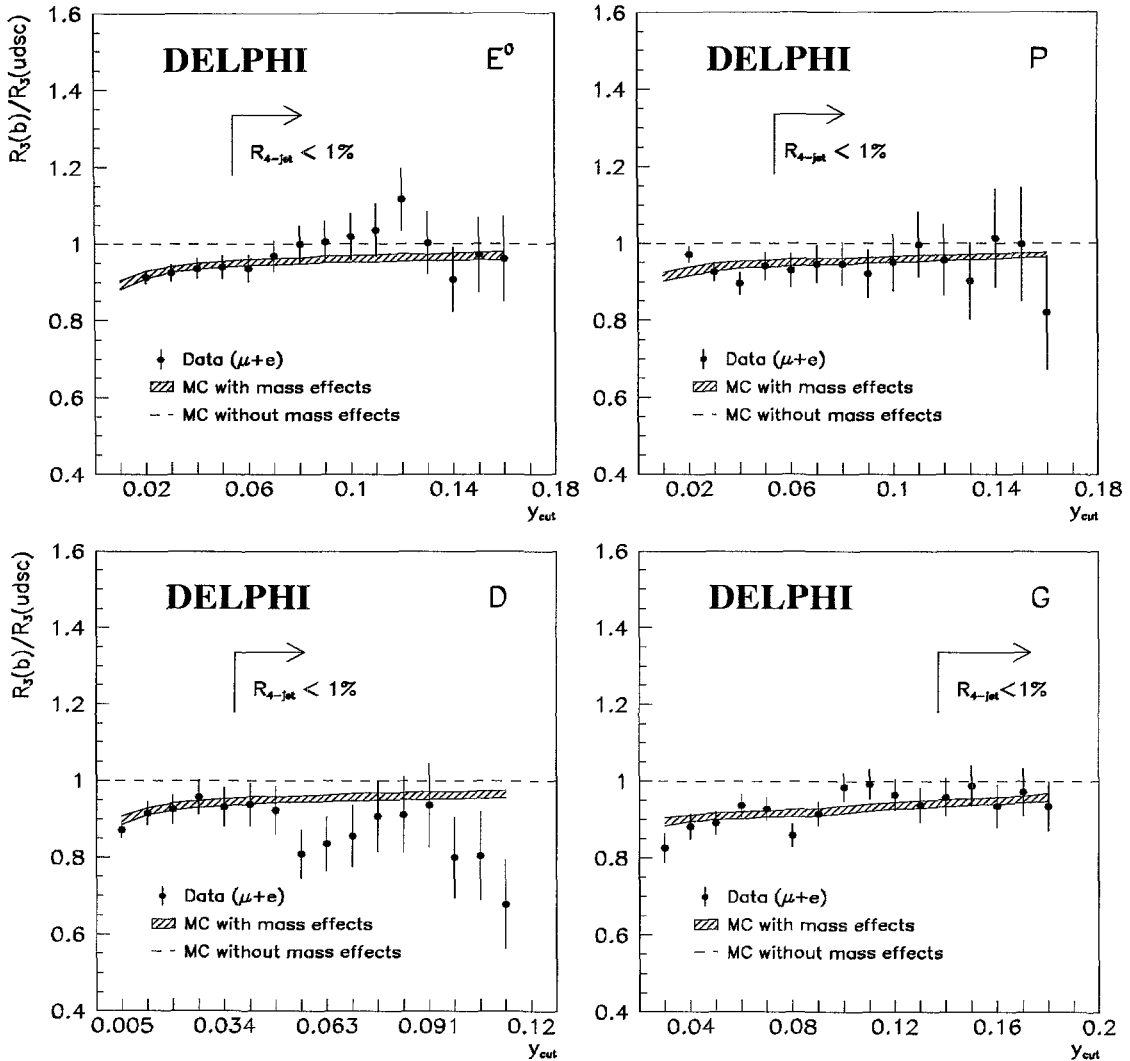


Fig. 1. The ratio R_3^b/R_3^{udsc} corrected for hadronization and detector effects, as a function of y_{cut} for the different recombination schemes for the combined lepton data - (note the different abscissa scales). The error bars are statistical only. Also indicated is the value of y_{cut} at which point the four-jet rate falls below the 1% level. The dashed line at unity represents the expectation from a flavour independent strong coupling constant assuming massless quarks; the hatched area, on the other hand, encompasses the spread in values obtained when incorporating mass effects as described in the text. The uncertainty due to the limited number of Monte Carlo statistics in the computation of the mass effects is also taken into account.

tree level calculations of ref. [23]. As these calculations do not include the complete $O(\alpha_s^2)$ corrections to the three-jet rate cross section, different approaches to their implementation were tried. As a first approximation, the mass corrections to $O(\alpha_s)$ only were directly applied. A second, more appropriate approach, was to weight the $O(\alpha_s)$ and $O(\alpha_s^2)$ predictions for

massive quarks by the multi-jet cross-sections given by either of the massless Matrix Elements or the Parton Shower Monte Carlo generators of ref. [18]. The hatched area in fig. 1 encompasses the spread in values obtained when incorporating the mass effects in these different ways; a comparison with the data points illustrates the significant effect of the b quark mass on

the multi-jet cross section.

Systematic uncertainties were then investigated using the numbers obtained within the E^0 scheme and for a value of y_{cut} of 0.06, which has the experimentally favoured property of yielding a large three-jet fraction for a given four-jet rate of approximately 0.5% [14]. At lower y_{cut} values, where the four-jet rate becomes significant, the $O(\alpha_s^2)$ calculations at scale values of $\mu^2 = s$ are known not to give a good description of the experimental multi-jet rate [15,26].

(1) The size of the uncertainty due to hadronization effects was evaluated by determining the hadronization correction factors using the Monte Carlo Parton Shower model with different fragmentation tunings. Specifically, the mean value of $x_E = E_{\text{hadron}}/E_{\text{beam}}$ for primordial b flavoured hadrons was varied in the range $0.68 \leq \langle x_E(b) \rangle \leq 0.74$ [11,19,20,27] by adjusting the ϵ_b parameter of the Peterson fragmentation function [28]; in addition, parameters of the Lund fragmentation function [29] for the $udsc$ quarks were varied in a range compatible with tuned values [30].

(2) The stringent p and p_T^{exc} cuts applied in order to achieve a b enriched sample of events severely reduced the number of Monte Carlo events for the computation of the detector and hadronization correction factors. The uncertainty introduced by the limited Monte Carlo statistics proved to be one of the main contributions to the overall systematic error.

(3) The uncertainties due to the errors on the percentages, P_i^q , in the inclusive lepton samples and the correction terms, C_i , were also considered. The latter uncertainty was found to be particularly significant owing to the large correction factors applicable to the contributions from background processes.

(4) The experimental error was obtained by repeating the analysis for a variety of cuts on the polar angle of the thrust axis. Any deviation outside expectations from statistical fluctuations was assigned to the systematic error.

(5) Finally, a small systematic error was assigned due to the uncertainty inherent in implementing the mass corrections.

The magnitudes of these uncertainties are listed in table 2. The final values (using the E^0 scheme with $y_{\text{cut}} = 0.06$) with their statistical and systematic errors, corrected for mass effects, are:

$$\mu (1990) :$$

Table 2

Systematic effects on the experimental measurement of R_3^b/R_3^{udsc} (method 1). A common systematic uncertainty of ± 0.03 is estimated within the muon samples, mainly from the background processes contributing to the β , γ terms of (3). Systematics (1), (4) and (5) are also common to the muon and electron samples.

Systematic	$\Delta (R_3^b/R_3^{udsc})$		
	1990 μ	1991 μ	1991 e
(1) hadronization	± 0.01	± 0.01	± 0.01
(2) MC statistics	± 0.08	± 0.04	± 0.05
(3) β , γ terms	± 0.05	± 0.04	± 0.05
(4) detector effects	± 0.01	± 0.01	± 0.01
(5) mass corrections	± 0.01	± 0.01	± 0.01
total (1) to (4)	± 0.10	± 0.06	± 0.07

$$\frac{R_3^b}{R_3^{udsc}} = 1.01 \pm 0.08 (\text{stat.}) \pm 0.10 (\text{syst.}),$$

$\mu (1991) :$

$$\frac{R_3^b}{R_3^{udsc}} = 0.99 \pm 0.05 (\text{stat.}) \pm 0.06 (\text{syst.}),$$

$e (1991) :$

$$\frac{R_3^b}{R_3^{udsc}} = 0.91 \pm 0.08 (\text{stat.}) \pm 0.07 (\text{syst.}).$$

A weighted average of the above measurements, taking into account the common systematic errors outlined in table 2, gives

$$\frac{R_3^b}{R_3^{udsc}} = 0.97 \pm 0.04 (\text{stat.}) \pm 0.04 (\text{syst.}).$$

In first order QCD, the three-jet rate is directly proportional to the strong coupling constant, i.e. $R_3 \propto \alpha_s$. The ratio R_3^b/R_3^{udsc} is therefore a direct measure of the relative strength of the coupling constants. It has been verified that the influence of second order QCD corrections to the relation between R_3^b/R_3^{udsc} and $\alpha_s^b/\alpha_s^{udsc}$ does not significantly affect the determination of the relative coupling strengths within the present statistical accuracy of the experiment, particularly when small energy scales ($\mu^2 \sim y_{\text{cut}}s$) in the second order QCD expression are considered. The ratio for the relative strength of the coupling constants is thus determined to be

$$\frac{\alpha_s^b}{\alpha_s^{udsc}} = 0.97 \pm 0.04 (\text{stat.}) \pm 0.04 (\text{syst.}).$$

4.2. method 2: fitting the lepton p and p_T distribution in two- and three-jet events

In the second method, rather than applying stringent cuts to obtain an enriched sample of b events, the predicted shapes of the lepton spectra from the processes $i = 1$ to 6 were used to fit the corresponding p and p_T^{inc} distributions of the data. Here, the momentum range considered was $4 < p(\mu) < 35$ GeV/ c for muons, and $3 < p(e) < 30$ GeV/ c for electrons.

The analysis proceeded first by deducing from the Monte Carlo simulation the two-dimensional p and p_T^{inc} probability distributions for each of the sources of prompt and background leptons. These are taken separately for two- and three-jet events at parton level leading to two- or three-jets at detector level. To help obtain smooth distributions, dedicated samples of inclusive lepton simulation events were generated. The probability distributions are thus denoted by

$$\rho_i^{mn},$$

where m is the number of jets at parton level, n the number of jets reconstructed at detector level, and i refers to the six categories of lepton candidates. The value of y_{cut} was chosen such that the fraction of four-jets at parton level is not greater than 1%. These were grouped with the three-jet events. A correction was later made for their contribution to the $m = 3$ sample when computing α_s^b . For the prompt leptons, the probability distributions, $\rho_{i=1,4}^{mn}$, were constructed as a function of fragmentation variable, z [22]; this allowed the heavy quark fragmentation functions to be fitted.

Next the data were binned in p and p_T^{inc} space for two- and three (or more)-jet event samples and fitted simultaneously by a maximum likelihood method to the functions $F(n\text{-jet})$:

$$F(2\text{-jet}) = \sum_{i=1,6} (N_i^2 f_i^{22} \rho_i^{22} + N_i^3 f_i^{32} \rho_i^{32}),$$

$$F(3\text{-jet}) = \sum_{i=1,6} (N_i^3 f_i^{33} \rho_i^{33} + N_i^2 f_i^{23} \rho_i^{23}).$$

N_i^m gives the total number of m -jet events at parton level of type i , and f_i^{mn} is a fraction that gives the probability of an n -jet event at detector level to have originated from an m -jet event at parton level, such that

$$f_i^{22} + f_i^{23} = 1 \text{ and } f_i^{32} + f_i^{33} = 1.$$

The corrections due to detector and hadronization effects, obtained using the Monte Carlo simulation model and calculated as a function of z for processes $i = 1, 4$, are therefore incorporated into these fractions.

The free parameters in the fit are α_s^b , the total number of b events (or equivalently the product branching ratio $\text{BR}(Z \rightarrow b\bar{b}) \times \text{BR}(b \rightarrow \mu, e)$), and ϵ_b of the Peterson fragmentation function [28]. Together, these parameters control the entries $N_{i=1,3}^m$ and their respective detection efficiencies (which themselves are a function of z), the shapes of the probability distributions, $\rho_{i=1,3}^{mn}$, and the fractions $f_{i=1,3}^{mn}$. In calculating the cascade contribution to the inclusive lepton signal, the ratio of the branching ratios $\text{BR}(b \rightarrow c \rightarrow \mu, e) / \text{BR}(b \rightarrow \mu, e)$ was taken to be 1.0 ± 0.2 [31], and the product branching ratio $b \rightarrow \tau \rightarrow \mu, e$ was taken as 0.9% [32,33]. The contribution from charm (i.e. $N_{i=4}^m$, $\rho_{i=4}^{mn}$ and $f_{i=4}^{mn}$) is likewise governed by α_s^c , the total number of c events (or equivalently the product branching ratio $\text{BR}(Z \rightarrow c\bar{c}) \times \text{BR}(c \rightarrow \mu, e)$), and ϵ_c , while the amount of background from misidentification and decays is determined by N_5^m and N_6^m respectively. However, owing to the large overlap between the charm and background distributions in p and p_T^{inc} space, no significant result for charm is obtained. The charm contribution was therefore fixed to the Standard Model prediction (with $\text{BR}(c \rightarrow \mu) = 9\%$ [34]), and $\alpha_s^c(M_{Z^0})$ set to the current world average α_s value of 0.118 [2], while the number of background events from misidentification and decays was allowed to vary.

For the α_s determination there is a dependence on the choice of renormalization scale, $x_\mu = \mu^2/s$ (here μ denotes the energy scale); $\alpha_s^b(M_{Z^0})$ was therefore determined as a function of the scale in the range $0.003 \leq x_\mu \leq 1$, which corresponds to a choice of μ in the range between the b quark mass and Z^0 mass. The quoted value of $\alpha_s(M_{Z^0})$ is then the arithmetic mean of the two most extreme values; an error due to the scale uncertainty is assigned by taking half the difference between the two extreme values. The results have also been corrected for the small contamination of four-jet events in the three-jet ($m = 3$) sample (at parton level), for initial state radiation and for the b quark mass [23]. The latter correction amounted

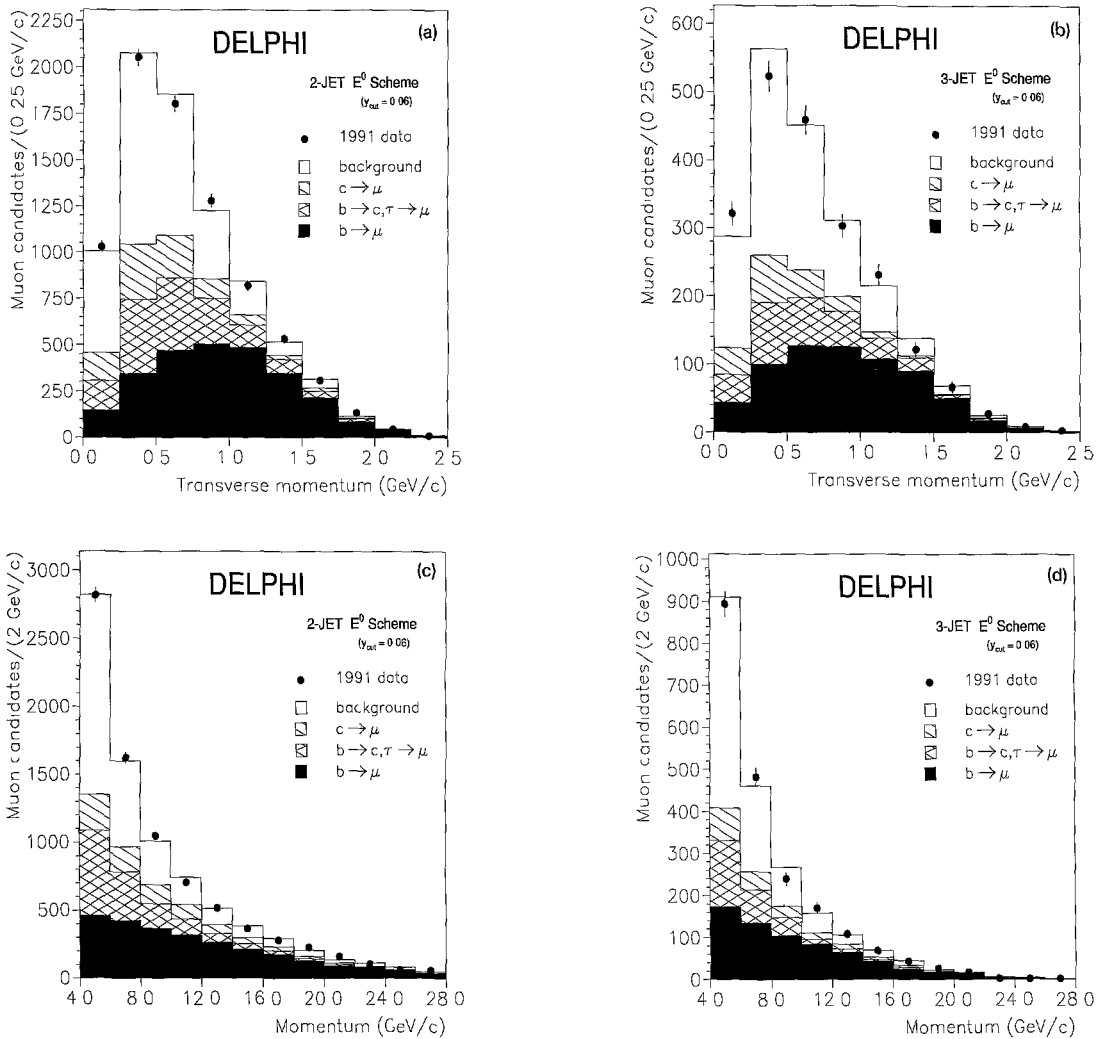


Fig. 2 (a) The p_T^{mc} distribution of muon candidates in the 1991 two-jet hadronic data within the range $4 < p(\mu) < 35$ GeV/c, together with the predictions of the fit. (b) The p_T^{mc} distribution of muon candidates in the 1991 three-jet hadronic data within the range $4 < p(\mu) < 35$ GeV/c, together with the predictions of the fit. (c) The p distribution of muon candidates in the 1991 two-jet hadronic data, together with the predictions of the fit. (d) The p distribution of muon candidates in the 1991 three-jet hadronic data, together with the predictions of the fit.

to a change in α_s^b of about +4% when using the E^0 recombination scheme with $y_{cut} = 0.06$. Fig. 2 shows the $p(\mu)$, $p_T^{mc}(\mu)$ distribution of the 1991 n -jet data, together with the results of the fit.

A number of sources of systematic uncertainties were investigated. These, together with their estimated errors, are listed in table 3, and are as follows:

- (1) The contributions to the inclusive lepton sam-

ple from background processes were varied by $\pm 15\%$ from the fitted values, while the contribution from charm was left free. The contributions from Dalitz decays of the π^0 , and from photon conversions in the DELPHI material, were further varied by $\pm 50\%$ in the inclusive electron sample. These variations resulted in a large change for charm, but had only a small effect on α_s^b .

Table 3

Systematic errors (rounded to the most significant decimal place) on the experimental measurement of α_s^b (method 2). The errors due to (1) to (4), (8) and (9) are common to the two inclusive muon samples, and lead to a common systematic uncertainty of ± 0.003 . Systematics (2), (3), (8) and (9) are largely common to the muon and electron samples, from where a common uncertainty of ± 0.002 is estimated.

Systematic	$\Delta \alpha_s^b$		
	1990 μ	1991 μ	1991 e
(1) background	± 0.002	± 0.002	± 0.002
(2) charm, ϵ_c, α_s^c	± 0.001	± 0.001	± 0.001
(3) bottom, fragmentation	± 0.001	± 0.001	± 0.001
(4) lepton detection eff.	± 0.001	± 0.001	± 0.001
(5) details of fit	± 0.002	± 0.001	± 0.002
(6) kinematic cuts	± 0.002	± 0.001	± 0.001
(7) p_T definition	± 0.002	± 0.002	± 0.002
(8) detector effects	± 0.001	± 0.001	± 0.001
(9) mass corrections	± 0.001	± 0.001	± 0.001
total (1) to (9)	± 0.005	± 0.004	± 0.005
(10) renormalization scale	± 0.008	± 0.009	± 0.008

(2) The contribution from charm was varied by changing the product branching ratio $\text{BR}(Z \rightarrow c\bar{c}) \times \text{BR}(c \rightarrow \mu, e)$ by $\pm 25\%$, by allowing the ϵ_c parameter to vary such that $0.48 \leq \langle x_E(c) \rangle \leq 0.56$ [20,35], and by changing the value of α_s^c by $\pm 30\%$. Large differences in the fitted level of background were seen, but the effects on α_s^b were small.

(3) The contribution from bottom was likewise varied by changing the product branching ratio $\text{BR}(Z \rightarrow b\bar{b}) \times \text{BR}(b \rightarrow \mu, e)$ by $\pm 10\%$ from the fitted value (which was in excellent agreement with published values [11,19–21]); the uncertainty in the contribution from the cascade decays was studied by varying the ratio $\text{BR}(b \rightarrow c \rightarrow \mu, e) / \text{BR}(b \rightarrow \mu, e)$ by $\pm 20\%$. These changes, however, had little impact on the α_s^b measurements. The fit was repeated using several other forms for the fragmentation function [29,36]; these not only influence the momentum spectra of leptons from direct and indirect b decay, but, in addition, influence the hadronization corrections that are applied. Only small deviations in α_s^b were, however, apparent. Typical values of $\langle x_E(b) \rangle$ were in the order of 0.71 to 0.73, in agreement with published values [11,19,20,27].

(4) The result for α_s^b was found to be slightly sen-

sitive to changes of $\pm 2\%$ in the relative lepton detection efficiencies for two- and three-jet events.

(5) Systematic effects due to details of the fit were investigated by repeating the fit with different binning. The results for α_s^b were found to be relatively stable.

(6) The influence of kinematic cuts was also investigated. Fits were repeated with the lower cuts varied over the range 3 to 5 GeV/c for p , and 0 to 0.5 GeV/c for p_T^{mc} ; only small deviations outside expectations from statistical fluctuations were evident.

(7) The fit was repeated with different definitions of the transverse momentum. In computing p_T^{mc} , the value of d_{join} in the LUCLUS algorithm was altered to 4.0 GeV/c; in another fit, p_T^{mc} was measured with respect to the jet axis computed by the E^0 jet finding algorithm with $y_{\text{cut}} = 0.02$; in a third fit, p_T^{exc} , as used in method 1, was chosen. The changes in α_s^b due to these various p_T definitions were incorporated in the systematic error.

(8) To investigate the effects of possible deficiencies in the simulation of the detector, fits were repeated using tighter cuts on the polar angle of the thrust axis.

(9) A systematic error due to the uncertainty in the size of the mass corrections was also applied.

(10) Finally, a systematic error was assigned due to the uncertainty inherent in the choice of renormalization scale.

As a further consistency check, fits were also repeated with y_{cut} values of 0.05 and 0.07; the results obtained were in good agreement.

The results quoted, in $O(\alpha_s^2)$ and at the M_{Z^0} scale, are

μ (1990) :

$$\alpha_s^b = 0.126$$

$$\pm 0.009 \text{ (stat.)} \pm 0.005 \text{ (syst.)} \pm 0.009 \text{ (scale) ,}$$

μ (1991) :

$$\alpha_s^b = 0.115$$

$$\pm 0.006 \text{ (stat.)} \pm 0.004 \text{ (syst.)} \pm 0.008 \text{ (scale) ,}$$

e (1991) :

$$\alpha_s^b = 0.117$$

$$\pm 0.009 \text{ (stat.)} \pm 0.005 \text{ (syst.)} \pm 0.008 \text{ (scale)}.$$

Combining the above measurements, taking account of the common systematic uncertainties outlined in table 3, the final result quoted, at the M_{Z^0} scale is

$$\alpha_s^b = 0.118$$

$$\pm 0.004 \text{ (stat.)} \pm 0.003 \text{ (syst.)} \pm 0.008 \text{ (scale)}.$$

A comparison with α_s for all flavours as measured from the three-jet fraction of all the hadronic events, $R_3(\text{had})$, further allowed the b coupling strength to be expressed in terms relative to that for the $udsc$ quarks. Such a comparison has the advantage of cancelling certain common systematic errors, in particular that due to the scale.

For a value of $y_{\text{cut}} = 0.06$ within the E^0 recombination scheme, using 1990 and 1991 data, α_s , in second order [16] and corrected for mass effects [23], is measured for all flavours at the M_{Z^0} scale to be

$$\alpha_s^{udscb} = 0.118$$

$$\pm [< 0.001] \text{ (stat.)} \pm 0.002 \text{ (syst.)} \pm 0.008 \text{ (scale)},$$

where the systematic error includes uncertainties in the hadronization process and detector acceptance. This result is in excellent agreement with that obtained from a multi-jet analysis appearing in a previous publication [3].

The relative coupling strengths are thus computed to be

$$\frac{\alpha_s^b}{\alpha_s^{udsc}} = 1.00 \pm 0.04 \text{ (stat.)} \pm 0.03 \text{ (syst.)}.$$

5. Summary

The strong coupling constant for b quarks has been determined from a multi-jet analysis of a total of 356 000 hadronic events, and that subset containing leptons. An analysis based on a comparison of the three-jet fraction in a b enriched sample of events (selected by requiring leptons with large p and p_T^{exc}) to that of all hadronic events, yielded

$$\frac{\alpha_s^b}{\alpha_s^{udsc}} = 0.97 \pm 0.04 \text{ (stat.)} \pm 0.04 \text{ (syst.)}$$

$$\text{[method 1]}.$$

A study of the predicted ratio R_3^b/R_3^{udsc} as a function of y_{cut} , for different recombination schemes, further illustrated the significance of the effect of the b quark mass on the multi-jet cross section [23].

By fitting the p and p_T^{exc} spectra of the lepton candidates in both two- and three-jet event samples simultaneously, using the spectra predicted from the Monte Carlo simulation for b , c and background events, a measurement of α_s^b at the Z^0 mass scale, in $O(\alpha_s^2)$, was obtained:

$$\alpha_s^b = 0.118$$

$$\pm 0.004 \text{ (stat.)} \pm 0.003 \text{ (syst.)} \pm 0.008 \text{ (scale)}.$$

A comparison with α_s for all flavours as measured from the corrected three-jet rate in the hadronic event sample enabled a measurement of the relative strength of the coupling constants, thereby cancelling some of the common systematic errors, in particular the scale error

$$\frac{\alpha_s^b}{\alpha_s^{udsc}} = 1.00 \pm 0.04 \text{ (stat.)} \pm 0.03 \text{ (syst.)}$$

$$\text{[method 2]}.$$

The two methods, which are subject to different systematic uncertainties, give results that are in gratifying agreement.

The results presented are in agreement with those of ref. [8], and verify the flavour independence of the strong coupling constant as predicted by QCD.

Acknowledgement

We are greatly indebted to our technical collaborators and to the funding agencies for their support in building and operating the DELPHI detector, and to the members of the CERN-SL Division for the excellent performance of the LEP collider. We also extend our thanks to A. Ballestrero, E. Maina and S. Moretti for providing us with their Monte Carlo generator, and acknowledge fruitful discussions, with them and with T. Sjöstrand, on the effect of massive quarks on the multi-jet cross section.

References

- [1] S. Bethke and J.E. Pilcher, *Ann. Rev. Nucl. Part. Sci.* 42 (1992) 251, and references therein;
T. Hebbeker, *Phys. Rep.* 217 (1992) 69, and references therein.
- [2] S. Bethke, Heidelberg preprint HD-PY 92/13 (1992), to appear in *Proc. of the XXVIth Int. Conf. on High Energy Physics, Dallas, Texas, USA (1992)*.
- [3] DELPHI Collab., P. Abreu et al., *Z. Phys. C* 54 (1992) 55.
- [4] OPAL Collab., P.D. Acton et al., *Z. Phys. C* 55 (1992) 1, CERN-PPE/93-38 (1993) to be published in *Z. Phys. C* ;
ALEPH Collab., D. Decamp et al., *Phys. Lett. B* 284 (1992) 163;
L3 Collab., B. Adeva et al., *Phys. Lett. B* 284 (1992) 471;
DELPHI Collab., P. Abreu et al., CERN-PPE/93-43 (1993) to be published in *Z. Phys. C* .
- [5] TASSO Collab., M. Althoff et al., *Phys. Lett. B* 138 (1984) 317;
TASSO Collab., W. Braunschweig et al., *Z. Phys. C* 42 (1989) 17; 44 (1989) 365,
G. Eckerlin, Ph.D. Thesis, University of Heidelberg, (1990).
- [6] W. Kwong, P.B. Mackenzie, R. Rosenfeld and J.L. Rosner, *Phys. Rev. D* 37 (1988) 3210.
- [7] T. Hebbeker, Aachen preprint PITHA 91/11 (1991).
- [8] L3 Collab., B. Adeva et al., *Phys. Lett. B* 271 (1991) 461.
- [9] DELPHI Collab., P. Aarnio et al., *Nucl. Instr. Meth.* A303 (1991) 233.
- [10] DELPHI Collab., P. Abreu et al., *Nucl. Phys. B* 367 (1991) 511.
- [11] DELPHI Collab., P. Abreu et al., *Z. Phys. C* 56 (1992) 46.
- [12] J. Buytaert et al., *Nucl. Instr. Meth. A* 310 (1991) 596,
DELPHI Collab., P. Abreu et al., *Phys. Lett. B* 276 (1992) 536;
N. Crosland, P. Kluit and G. Wilkinson, DELPHI Internal Note, DELPHI 92-17 PROG 157 (1992).
- [13] DELPHI Collab., P. Abreu et al., *Phys. Lett. B* 301 (1993) 145;
M. Calvi, F.R. Cavallo and C. Matteuzzi, DELPHI Internal Note, DELPHI 91-38 PROG 173 (1991).
- [14] S. Bethke, Z. Kunszt, D. Soper and W.J. Stirling, *Nucl. Phys. B* 370 (1992) 310.
- [15] JADE Collab., W. Bartel et al., *Z. Phys. C* 33 (1986) 23;
JADE Collab., S. Bethke et al., *Phys. Lett. B* 213 (1988) 235
- [16] Z. Kunszt and P. Nason, CERN Report CERN/89-08 (1989) Vol. 1, p. 373.
- [17] S. Catani et al., *Phys. Lett. B* 269 (1991) 2432;
N. Brown and W.J. Stirling, *Z. Phys. C* 53 (1992) 629.
- [18] T. Sjostrand, *Comp. Phys. Comm.* 39 (1986) 346;
T. Sjostrand and M. Bengtsson, *Comp. Phys. Comm.* 43 (1987) 367.
- [19] L3 Collab., B. Adeva et al., *Phys. Lett. B* 241 (1990) 416; *Phys. Lett. B* 261 (1991) 177;
OPAL Collab., P.D. Acton et al., *Z. Phys. C* 55 (1992) 191.
- [20] ALEPH Collab., D. Decamp et al., *Phys. Lett. B* 244 (1990) 551;
OPAL Collab., M.Z. Akrawy et al., *Phys. Lett. B* 263 (1991) 311.
- [21] MARK II Collab., J.F. Kral et al., *Phys. Rev. Lett.* 64 (1990) 1211;
DELPHI Collab., P. Abreu et al., *Phys. Lett. B* 281 (1992) 383.
- [22] J. Chrin, Manchester preprint, MAN-HEP/90-02 (1990).
- [23] A. Ballestrero, E. Maina and S. Moretti, *Phys. Lett. B* 294 (1992) 425; Torino preprint DFTT 92/53 (1992).
- [24] B.L. Ioffe, *Phys. Lett. B* 78 (1978) 277.
- [25] R. Kleiss, W.J. Stirling and S.D. Ellis, *Comp. Phys. Comm.* 40 (1986) 359.
- [26] TASSO Collab., W. Braunschweig et al., *Phys. Lett. B* 214 (1988) 235;
OPAL Collab., M. Z. Akrawy et al., *Phys. Lett. B* 235 (1990) 389; *Z. Phys. C* 49 (1991) 375; DELPHI Collab., P. Abreu et al., *Phys. Lett. B* 247 (1990) 167;
L3 Collab., B. Adeva et al., *Phys. Lett. B* 248 (1990) 464;
JADE Collab., N. Magnussen et al., *Z. Phys. C* 49 (1991) 29.
- [27] L3 Collab., O. Adriani et al., *Phys. Lett. B* 288 (1992) 412;
DELPHI Collab., P. Abreu et al., *Z. Phys. C* 57 (1993) 181.
- [28] C. Peterson, D. Schlatter, I. Schmitt and P.M. Zerwas, *Phys. Rev. D* 27 (1983) 105.
- [29] B. Anderson, G. Gustafson and B. Soderberg, *Z. Phys. C* 20 (1983) 317.
- [30] OPAL Collab., M.Z. Akrawy et al., *Z. Phys. C* 47 (1990) 505;
L3 Collab., B. Adeva et al., *Phys. Lett. B* 257 (1991) 469; *Z. Phys. C* 55 (1992) 39;
W. de Boer and H. Furstenuau, Karlsruhe preprint IEKP-KA/91-07 (1991);
ALEPH Collab., D. Decamp et al., *Z. Phys. C* 55 (1992) 209.
- [31] CLEO Collab., S. Henderson et al., *Phys. Rev. D* 45 (1992) 2212
- [32] C. Quigg and J.L. Rosner, *Phys. Rev. D* 19 (1979) 1532,
J.P. Leveille, *Proc. of the 2nd Moriond Workshop*,

- Les Arcs, Savoie, France (1982) p 191;
P. Heiliger and L.M. Sehgal, Phys. Lett. B 229 (1989) 409;
ALEPH Collab., D. Buskulic et al., Phys. Lett. B 298 (1993) 479.
- [33] Particle Data Group, K. Hikasa et al., Phys. Rev. D 45 (1992) S1.
- [34] JADE Collab., W. Bartel et al., Z. Phys. C 33 (1987) 33, and references therein;
ARGUS Collab., H. Albrecht et al., Phys. Lett. B 278 (1992) 202, and references therein
- [35] OPAL Collab., G. Alexander et al., Phys. Lett. B 262 (1991) 341;
- ALEPH Collab., D. Decamp et al., Phys. Lett. B 266 (1991) 218;
DELPHI Collab., P. Abreu et al., A Measurement of D Meson Production in Z^0 Hadronic Decays, to be submitted.
- [36] V.G. Kartvelishvili, A.K. Likhoded and V.A. Petrov, Phys. Lett. B 78 (1978) 615,
M.G. Bowler, Z. Phys. C 11 (1981) 169,
P.D.B. Collins and T.P. Spiller, J. Phys. G: Nucl. Phys. 11 (1985) 1289,
D.A. Morris, Nucl. Phys. B313 (1989) 634;
T. Sjostrand, CERN-TH/92-6488 (1992) p. 202.